Since January 2020 Elsevier has created a COVID-19 resource centre with free information in English and Mandarin on the novel coronavirus COVID-19. The COVID-19 resource centre is hosted on Elsevier Connect, the company's public news and information website.

Antiviral Research 179 (2020) 104817

Contents lists available at ScienceDirect

Antiviral Research

journal homepage: www.elsevier.com/locate/antiviral

Research paper

Imiquimod suppresses respiratory syncytial virus (RSV) replication via PKA pathway and reduces RSV induced-inflammation and viral load in mice lungs

Franco Maximiliano Salinas[a,b,1], Antonela Díaz Nebreda[c,1], Luciana Vázquez[d], María Virginia Gentilini[e], Victoria Marini[a], Martina Benedetti[a], Mercedes Soledad Nabaes Jodar[f,g], Mariana Viegas[f,g], Carina Shayo[c], Carlos Alberto Bueno[a,b,*]

[a] Universidad de Buenos Aires, Facultad de Ciencias Exactas y Naturales, Departamento de Química Biológica, Laboratorio de Virología, Buenos Aires, Argentina
[b] CONICET - Universidad de Buenos Aires, Instituto de Química Biológica de la Facultad de Ciencias Exactas y Naturales (IQUIBICEN). Buenos Aires, Argentina
[c] Laboratorio de Patología y Farmacología Molecular, Instituto de Biología y Medicina Experimental, IBYME, CONICET, Buenos Aires, Argentina
[d] Unidad Operativa Centro de Contención Biológica (UOCCB) - Administración Nacional de Laboratorios e Institutos de Salud (ANLIS), Argentina
[e] Instituto de Medicina Traslacional, Trasplante y Bioingeniería (IMETTYB)-CONICET, Buenos Aires, Argentina
[f] CONICET, Buenos Aires, Argentina
[g] Laboratorio de Virología, Hospital de Niños Ricardo Gutiérrez, Buenos Aires, Argentina

ARTICLE INFO

Keywords:
Respiratory syncytial virus (RSV)
Antiviral
Imiquimod
PKA
Toll like receptors (TLR)

ABSTRACT

Respiratory syncytial virus (RSV) is a leading cause of lower respiratory tract disease and bronchiolitis in children, as well as an important cause of morbidity and mortality in elderly and immunocompromised individuals. However, there is no safe and efficacious RSV vaccine or antiviral treatment. Toll Like Receptors (TLR) are important molecular mediators linking innate and adaptive immunity, and their stimulation by cognate agonists has been explored as antiviral agents. Imiquimod is known as a TLR7 agonist, but additionally acts as an antagonist for adenosine receptors. In this study, we demonstrate that imiquimod, but not resiquimod, has direct anti-RSV activity via PKA pathway in HEp-2 and A549 cells, independently of an innate response. Imiquimod restricts RSV infection after viral entry into the host cell, interfering with viral RNA and protein synthesis. Probably as a consequence of these anti-RSV properties, imiquimod displays cytokine modulating activity in RSV infected epithelial cells. Moreover, in a murine model of RSV infection, imiquimod treatment improves the course of acute disease, evidenced by decreased weight loss, reduced RSV lung titers, and attenuated airway inflammation. Consequently, imiquimod represents a promising therapeutic alternative against RSV infection and may inform the development of novel therapeutic targets to control RSV pathogenesis.

1. Introduction

Respiratory syncytial virus (RSV) is an important pathogen of the human respiratory tract (Borchers et al., 2013). RSV infection results in viral bronchiolitis in around 30% of infants who become infected and it can result in life-threatening severe bronchiolitis and viral pneumonia (Smyth and Openshaw, 2006). RSV causes significant mortality in the developing world, resulting in an estimated 200,000 annual deaths in young children globally, in addition to major morbidity (33.8 million episodes worldwide annually) (Nair et al., 2010). Besides, RSV is a leading cause of morbidity and mortality in elderly and immunocompromised individuals (Kwon et al., 2017).

Despite the prevalence of RSV bronchiolitis, there is no vaccine available and, apart from supportive measures, there is no specific effective treatment since routine use of bronchodilators or antiviral ribavirin has been proven to be of no significant benefit (Tregoning and Schwarze, 2010; Turner et al., 2014). Therefore, a clearer understanding of host defense factors that contribute to effective protection against RSV infection and disease is urgently needed and could provide substantial help to the development of novel therapeutic strategies.

During the early course of most viral infections, antiviral immunity is induced through pattern recognition receptors, such as Toll-like

* Corresponding author. CONICET - Universidad de Buenos Aires, Instituto de Química Biológica de la Facultad de Ciencias Exactas y Naturales (IQUIBICEN), C-1428GBA, Buenos Aires, Argentina.
E-mail address: cbueno@qb.fcen.uba.ar (C.A. Bueno).
[1] Equivalent contribution to this work.

https://doi.org/10.1016/j.antiviral.2020.104817
Received 26 December 2019; Received in revised form 31 March 2020; Accepted 2 May 2020
Available online 06 May 2020
0166-3542/

receptors (TLR), which stimulate the innate immune response. TLR can trigger cytokine secretion, dendritic cell maturation, and antigen presentation, which in turn can enhance the adaptive immune response (Uematsu and Akira, 2006). Because of this ability to induce innate and adaptive responses, TLR agonists have been explored as antiviral therapeutic agents. TLR3, TLR4, TLR7, TLR8 and TLR9 agonists have been successfully applied to nonhuman primate models of dengue virus and hepatitis B virus (HBV) and in murine models for influenza and herpes simplex virus (HSV) (Boivin et al., 2008; Zhang et al., 2009; Boukhvalova et al., 2010; Sariol et al., 2011; Shinya et al., 2011; Tuvim et al., 2012; Lanford et al., 2013; Lucifora et al., 2018; To et al., 2019). Particularly in the mouse model of RSV, prophylactic treatment with a TLR3 agonist not only reduces viral replication in the lungs, but also results in an amelioration of the clinical illness and a reduction in lung inflammation (Guerrero-Plata et al., 2005).

In order to provide further insight into the potential of TLR agonists to induce antiviral and immunomodulatory activities in RSV infections, the aim of the present study was to test the anti-RSV activity of different TLR agonists in epithelial cells. Moreover, we extended the testing for imiquimod (TLR7 agonist), in order to analyze its antiviral mode of action against RSV *in vitro*, as well as its effect on the production of different cytokines in RSV-infected epithelial and macrophages. Finally, we studied the activity of imiquimod against RSV infection in a murine model of pulmonary infection.

2. Materials and methods

2.1. Reagents

LPS (TLR4 ligand) from *Escherichia coli* serotype 055:B5, (−)-N6-(2-Phenylisopropyl) adenosine (R-PIA), dibutyryl cAMP (dbcAMP) and forskolin were obtained from Sigma. Pam2CSK4 (TLR2/TLR6 ligand), poly(I:C)-HMW (TLR 3 ligand), imiquimod (TLR7 ligand) and CpG ODN 2395 (TLR9 ligand) were purchased from InvivoGen. Resiquimod (TLR7/8 ligand) was kindly provided by Dr. Marianela Candolfi (INBIOMED-UBA-CONICET). Imiquimod was dissolved in water, according to the manufacturer's instructions. The rabbit monoclonal anti-Phospho-CREB (Ser133) (87G3) and anti-CREB (48H2) were purchased from Cell Signaling. KT5720 was obtained from Tocris Bioscience. The mouse monoclonal antibody anti-gF of RSV was obtained from US Biological Life Sciences. Secondary goat anti-mouse FluoroLinkTM CyTM3 antibodies were purchased from GE Healthcare. The peroxidase-conjugated goat anti-rabbit antibodies and Dapi for nucleic acid staining were obtained from Sigma.

2.2. Cells and viruses

The human HEp-2 cell line (human epidermoid cancer cell line) and the human A549 cell line (human lung carcinoma cell line) were grown in DMEM/F12 supplemented with 10% inactivated fetal bovine serum (FBS). Murine macrophage cell line J774A.1 was kindly provided by Dr. Osvaldo Zabal (INTA–Castelar, Buenos Aires, Argentina) and grown in RPMI1640 medium supplemented with 10% FBS. Vero cells were grown in MEM supplemented with 10% FBS. Human RSV strains A2 and line 19 were kindly provided by Dr. Laura Talarico (INFANT–Buenos Aires, Argentina). Working stocks of RSV were prepared as previously described (Salinas et al., 2019). Briefly, semiconfluent monolayers of HEp-2 cells were infected with RSV strains line 19 and A2 (multiplicity of infection (moi) = 0.2) and were incubated 3–4 days, monitoring the development of cytopathic effect (CPE) daily, until CPE ≥80% of cell monolayer, but still intact and attached to flask bottom. Then, supernatant was removed and 5 ml of cold 25% (w/v) sterile sucrose was added. Then the flask was transferred to −80 °C, being sure that cell surface is covered with sucrose solution while in the freezer. After three cycles of freezing and thawing, lysates were transferred to sterile 50 ml conical tubes. Cellular debris was removed by centrifugation at 500 × *g* and 4 °C for 10 min, and supernatants were aliquoted and stored at −80 °C until use. Sucrose in concentrations at 25% has a stabilizing effect and reduces loss of infectivity of this very labile virus. Virus titration was performed in Vero cells by plaque assay.

2.3. Antiviral activity

Cells grown in 24-well plates were infected with a multiplicity of infection (moi) of 1. After 1 h adsorption at 37 °C, the inoculum was removed and medium containing the compounds was added, in triplicate. The plates were incubated at 37 °C until 24 h p.i. After cell disruption by freezing and thawing, supernatants were titrated by plaque assay in Vero cells, and the effective concentration 50 (EC_{50}) was calculated as the concentration of compounds required to reduce viral yields by 50% relative to the untreated virus control, that were incubated with medium alone.

2.4. Cytotoxicity assay

Cell viability was determined using the tetrazolium salt MTT (3-(4,5-dimethylthiazol-2-yl)-2,5-diphenyltetrazolium bromide) (Sigma) according to the manufacturer's instructions. The cytotoxic concentration 50 (CC_{50}) is the concentration of compounds required to reduce cell viability by 50% relative to untreated cells, that are incubated with medium alone.

2.5. Virucidal effect

RSV line 19 and A2 (10^7 PFU) were diluted in culture medium containing or not each compound and incubated for 120 min at 37 °C. Aliquots were diluted to a non-inhibitory drug concentration and titrated by plaque assay in Vero cells.

2.6. Time-of-addition assays

For pre-infection assays, cells were treated with imiquimod during 2 h at 37 °C, washed with PBS and then infected with RSV A2 (moi = 1). For co-infection, cells were simultaneously infected with RSV A2 and treated with imiquimod. After 1 h adsorption at 37 °C, the virus-drug mixture was removed, washed and compound free medium was added. For post-infection (p.i.) assays, cells were infected with RSV for 1 h at 37 °C and then treated with the tested compound at 0, 2, 4, 6, 8, 12 and 16 h after infection. A control culture that was infected but not treated (CV) was simultaneously performed. Cells were further incubated at 37 °C till 24 h p.i., and after cell disruption by freezing and thawing, supernatants were titrated by plaque assay in Vero cells.

2.7. RSV qRT-PCR assay

At the indicated time points p.i./compound incubation, total RNAs were extracted from supernatants, after freezing and thawing the infected cells, with QIAamp® Viral RNA Mini Kit (QIAGEN, USA) according to the manufacturer's instructions. The first-strand cDNA synthesis was performed with SuperScript III Reverse Transcriptase (SSIII) (Thermo Fisher Scientific) following manufacturer's instructions and a primer which recognizes the M gene of the negative-strand RSV RNA genome. Then a quantitative PCR (qPCR) with primers and probe targeting the M gene previously reported (Kim et al., 2011) was performed with SensiFAST™ Probe No-ROX Kit (Bioline) following manufacturer's instructions. RNase P DNA was used as a reference gene and was amplified with the corresponding gene specific primers and probe and the qPCR was performed with SensiFAST™ Probe No-ROX Kit (Bioline). Average viral RNA Cq values were normalized to the average Cq values of RNase P and ΔΔCt based fold-change calculations were set relative to untreated-virus infected cells at 6 h p.i.

2.8. Immunofluorescence assay (IF) and semiquantitative IF analysis

Subconfluent cells grown on glass coverslips in 24-well plates were fixed with methanol for 10 min at −20 °C. After three washes with PBS, the coverslips were inverted on a drop of diluted primary antibody for 30 min at 37 °C, and then returned to culture dishes and subjected to three additional washes with PBS. Afterwards, cells were incubated with diluted secondary antibody for 30 min at 37 °C. Then, cells were subjected to three additional washes with PBS, and incubated with DAPI. Finally, coverslips were rinsed, mounted and photographed with an Olympus IX71 with epifluorescence optics. Percentage of cells expressing gF was calculated as the number of cells with gF fluorescence relative to the total cell number stained with DAPI, in at least 5 coverslips, performed in duplicate.

2.9. Western blot analysis

Whole extracts from cells grown in 24-well plates for 24 h were loaded on 10% sodium dodecyl sulphate-polyacrylamide gel electrophoresis (SDS-PAGE) and transferred onto polyvinylidene fluoride (PVDF) membranes for 60 min at 75 mA. Membranes were blocked in PBS containing 5% unfitted milk overnight and then incubated with diluted primary antibodies ON at 4 °C. After washing, membranes were incubated with diluted peroxidase conjugated antibodies for 1 h at 37 °C. The immunoreactive bands were visualized using an enhanced chemiluminescence system (Amersham ECL). CREB was used as loading control. Densitometric quantification was performed using Scion image. The protein level was calculated relative to CREB level, and then normalized to untreated cells, defined as 1.

2.10. Cytokine determination

Mouse TNF-α and IL-6, and Human IL-6 and IL-8 were quantified by commercial ELISA sets (BD OptEIATM, Becton–Dickinson) according to the manufacturer's instructions.

2.11. Pulmonary infection in mouse model

Animal studies were approved by the Comisión Institucional de Cuidado y Uso de Animales de Laboratorio (CICUAL) of the Facultad de Ciencias Exactas y Naturales, Universidad de Buenos Aires, Argentina. Female Balb/C mice were purchased from Facultad de Veterinaria, Universidad de Buenos Aires, Argentina. The animals were housed in an Animal Facility Biosafety Level 3 (ABSL-3) (UOCCB, ANLIS-Malbrán, Buenos Aires, Argentina) in individually ventilated cages and fed with food and water ad libitum for at least 1 week before experimental use at 6–8 week of age. Mice received 50 μl RSV line 19 and A2 (5×10^6 PFU) or 25% (w/v) sucrose (as described above, viral stocks were suspended in 25% (w/v) sucrose) by intranasal (i.n.) delivery under light general anesthesia (isoflurane) (6 per group). A total of 5 mg/kg of imiquimod (dissolved in water) or a vehicle (water) for control group, was given 1 h p.i. intranasally (i.n.). Mice further received a daily dose of 5 mg/kg of imiquimod until day 4 p.i. Body weights were monitored daily, and groups of mice were culled on day 4 or 8 p.i. Lungs from day 4 were removed, weighed, and used for titration of infectious virus. Briefly, snap frozen lungs were homogenized on ice using glass Dounce homogenizers. Tissue debris was pelleted by centrifugation at 4 °C for 10 min at 300 g and supernatants were immediately serially diluted in FBS free medium and titrated by plaque assay in Vero cells. The right lungs from day 8 were used for gene expression studies, and in parallel, the left lung was submerged in Bouin solution for fixation for 24 h and subsequent histological sectioning and staining. Lung sections were assessed for severity of inflammation by two independent observers, Dr. María Virginia Gentilini and Dr. Carlos Bueno, blinded to treatment. An index of pathologic changes in hematoxylin and eosin (H&E) slides was obtained accordingly to Zappia et al. (2019). Briefly, 20 consecutive airways per slide were examined at 400 × magnification and scoring the inflammatory infiltrates around the airways and vessels for severity (0, normal; 1, ≤3 cells diameter thick; 2, 4 to 10 cells diameter thick; 3, ≥10 cells diameter thick). The Inflammatory Index was calculated by dividing the sum of the airway scores from each lung by the number of airways examined.

2.12. Cytokines and cystatin A qRT-PCR

RNA from mouse lung tissue or human cell cultures were isolated using TRIzol reagent (Life Technologies) and reverse transcribed with ImProm-II™ Reverse Transcription System A3800 (Promega), according to the manufacturer's instructions. Quantitative PCR was performed on the Bio-Rad iQ5 real-time PCR system using FastStart SYBR green Master Mix reagent (Roche). β-actin was used as an internal control for normalization. The data were analyzed using the $2^{-\Delta\Delta Ct}$ formula. The sequences of the primers for gene expression were obtained from Primer Bank (Harvard Medical School; https://pga.mgh.harvard.edu/primerbank/) except for β-actin (human), and are listed (forward and reverse):

TNF-α mouse: F: CAGGCGGTGCCTATGTCTC; R: CGATCACCCCGAAGTTCAGTAG.

PrimerBank ID: 133892368c1 (https://pga.mgh.harvard.edu/primerbank/).

IL-6 mouse: F:TAGTCCTTCCTACCCCAATTTCC; R: TTGGTCCTTAGCCACTCCTTC.

PrimerBank ID: 13624311a1.

IL-4 mouse: F: GGTCTCAACCCCCAGCTAGT; R: GCCGATGATCTCTCTCAAGTGAT.

PrimerBank ID: 10946584a1.

IFN-γ mouse: F: ATGAACGCTACACACTGCATC; R: CCATCCTTTTGCCAGTTCCTC.

PrimerBank ID: 33468859a1(https://pga.mgh.harvard.edu/primerbank/).

IL-17 A mouse: F: TTTAACTCCCTTGGCGCAAAA; R: CTTTCCCTCCGCATTGACAC.

PrimerBank ID: 6754324a1 (https://pga.mgh.harvard.edu/primerbank/).

β-actin mouse: F: GTGACGTTGACATCCGTAAAGA; R: GCCGGACTCATCGTACTCC.

PrimerBank ID 145966868c1(https://pga.mgh.harvard.edu/primerbank/).

Cystatin A human: F:AAACCCGCCACTCCAGAAATC;

R: ACCTGCTCGTACCTTAATGTAG. Primer Bank ID: 61743964c1

β-actin human: F: GAGACCTTCAACACCCCAGCC; R: GGCCATCTCTTGCTCGAAGTC.

2.13. Transfections and reporter gene assays

Transfection assays with Lipofectamine 2000 reagent (Invitrogen) were performed according to the manufacturer's instructions. The NF-κB-LUC reporter vector and RSV-β- gal plasmid, coding for the bacterial β-galactosidase gene under the control of the viral RSV promoter, were kindly provided by Dr. Susana Silberstein (Universidad de Buenos Aires, Argentina). Reporter quantitation with Luciferase Assay System E1500 (Promega) and β-Galactosidase Enzyme Assay System E2000 (Promega) were performed according to the manufacturer's instructions.

2.14. Statistical analysis

EC_{50} was calculated from dose–response curves using the software GraphPad Prism 4.0. Statistical significance was assessed either using a one-way analysis of variance (ANOVA) followed by a Tukey's multiple comparison test, or a two-way ANOVA with Bonferroni's post test where appropriate. p-value < 0.05 was considered significant.

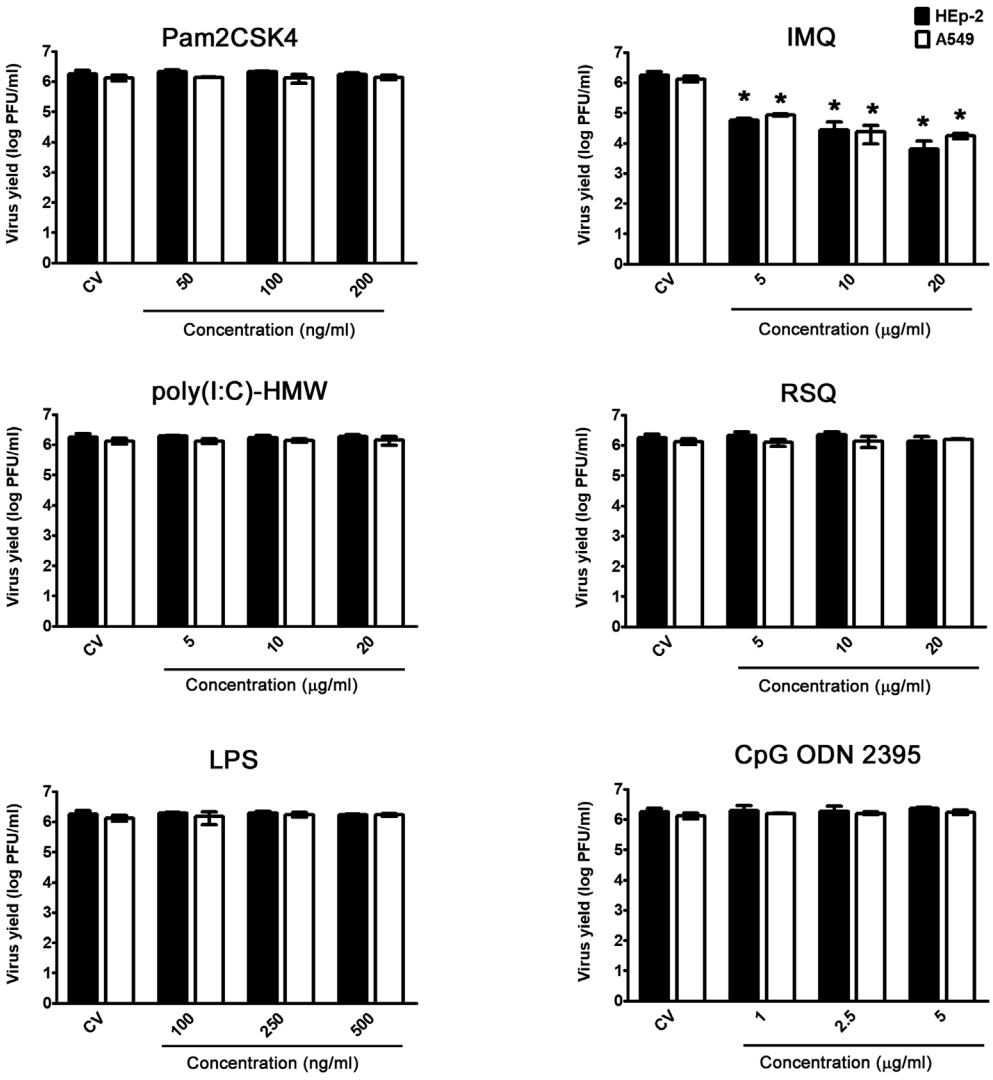

Fig. 1. Evaluation of the anti-RSV activity of TLR agonists *in vitro*. HEp-2 and A549 cells were infected with RSV A2 (moi = 1) for 1 h, and then treated with 50, 100 and 200 ng/ml of Pam2CSK4 (TLR 2/6 agonist), 5, 10 and 20 μg/ml of poly(I:C)-HMW (TLR 3 agonist), 100, 250 and 500 ng/ml of LPS (TLR 4 agonist), 5, 10 and 20 μg/ml of imiquimod (IMQ, TLR 7 agonist), 5, 10 and 20 μg/ml of resiquimod (RSQ, TLR 7/8 agonist) or 1, 2.5 and 5 μg/ml of CpG ODN 2395 (TLR 9 agonist) for 24 h. Total virus yields were determined by plaque assay in Vero cells. (CV): untreated–infected control cells. Data represent mean ± SD for n = 3 independent experiments, performed in duplicate. *Significantly different from CV (p-value < 0.05); One way ANOVA with Tukey post test.

Table 1
EC_{50} and SI of imiquimod against RSV line 19 and A2.

	HEp-2		A549		Vero	
	line 19	A2	line 19	A2	line 19	A2
EC_{50}	0.9 ± 0.5	0.8 ± 0.4	3.0 ± 0.9	2.1 ± 0.7	1.2 ± 0.4	1.5 ± 0.6
SI	55	62	17	24	42	33

EC_{50}: Effective Concentration 50. EC_{50} (μg/ml) were calculated by nonlinear regression.
SI: selectivity indices (ratio CC_{50}/CE_{50}). SI were calculated considering as CC_{50} the maximal concentration tested (50 μg/ml).
Data represent mean ± SD for n = 3 independent experiments, performed in triplicate.

3. Results

3.1. Evaluation of the anti-RSV effect of TLR agonists in vitro

To assess the effects of TLR stimulation on RSV infection, HEp-2 and A549 cells were infected with RSV A2 (moi = 1) and treated with different concentrations of Pam2CSK4 (TLR 2/6 agonist), poly(I:C)-HMW (TLR 3 agonist), LPS (TLR 4 agonist), imiquimod (IMQ, TLR 7 agonist), resiquimod (RSQ, TLR 7/8 agonist) or CpG ODN 2395 (TLR 9 agonist). These TLR agonists concentrations were chosen based on published data that demonstrate TLR stimulation in different cell types *in vitro* (Tissari et al., 2005; Kan et al., 2012; Bueno et al., 2015; Lucifora et al., 2018; Salinas et al., 2019). After 24 h, the amounts of infectious virus particles in the culture medium were decreased only by treatment with imiquimod, while the other TLR agonists did not affect viral replication at these concentrations tested (Fig. 1).

3.2. Antiviral activity of imiquimod against RSV in vitro

In order to confirm the anti-RSV activity of imiquimod, HEp-2, A549, and Vero cells were infected with RSV strains A2 and line 19 (moi = 1) and treated with different concentrations of imiquimod during 24 h (0.1–50-μg/ml), and the selectivity index (SI), the relationship between CC_{50} and EC_{50} values, was calculated. Imiquimod significantly reduced infectivity of both strains of RSV in a concentration-dependent manner (Table 1 and Fig. 2A). Besides, imiquimod had

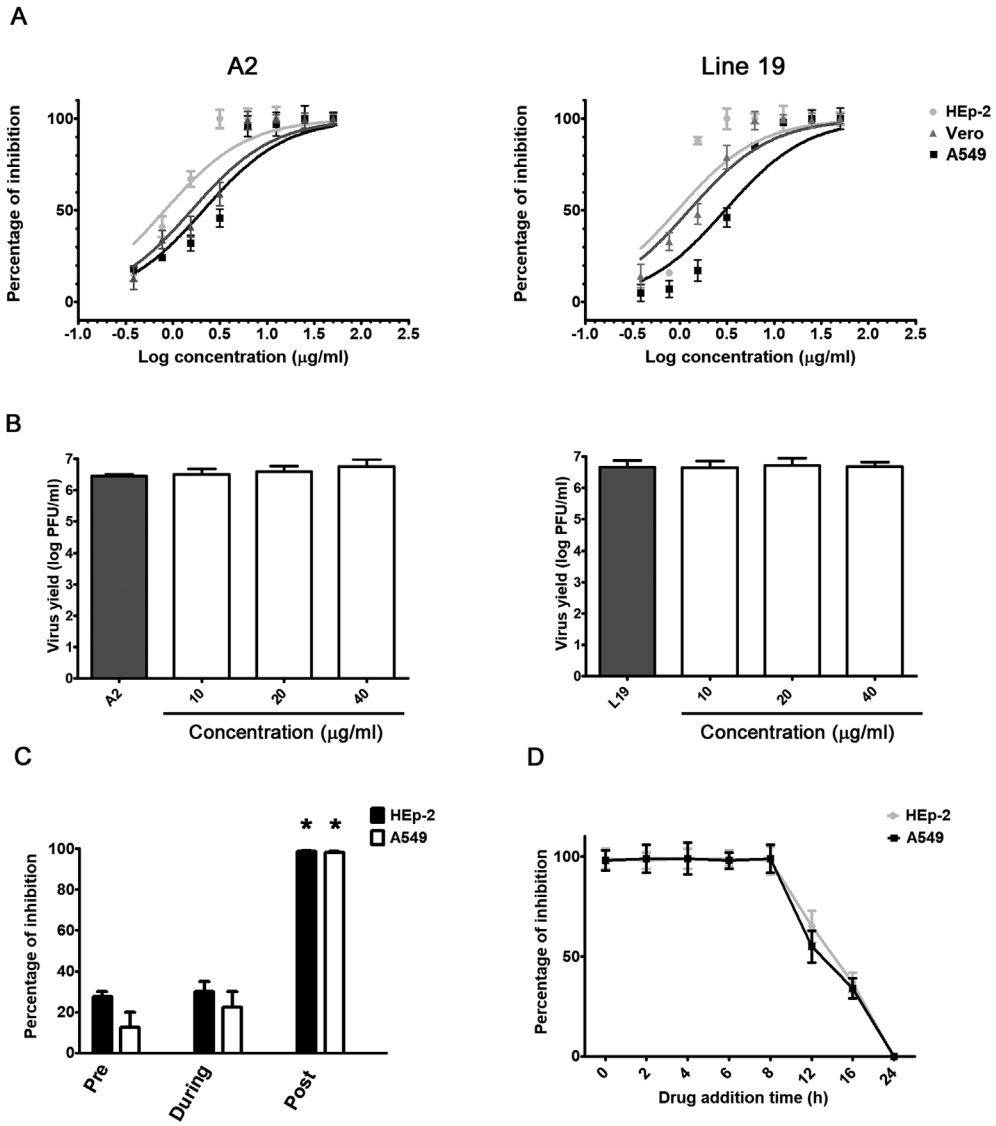

Fig. 2. Antiviral activity of imiquimod against RSV *in vitro*. (A) HEp-2, A549 and Vero cells were infected with RSV A2 and line 19 (moi = 1) and treated with different concentrations of imiquimod. After 24 h, total virus yields were titrated by plaque assay in Vero cells. (B) RSV A2 and line 19 were incubated with different concentrations of imiquimod for 2 h at 37 °C. Remaining infectivity was determined by plaque assay in Vero cells. (C) For pre-infection assays, HEp-2 and A549 cells were exposed or not to imiquimod (10 μg/ml) during 2 h, washed with PBS, and then infected with RSV A2 (moi = 1) during 24 h. For co-infection, cells were simultaneously infected with RSV A2 (moi = 1) and treated with imiquimod (10 μg/ml). After 1 h adsorption, the virus-drug mixture was removed, washed with PBS, and compound free medium was added during 24 h. For p.i. assays, cells were infected with RSV A2 (moi = 1) for 1 h, and then treated with imiquimod (10 μg/ml) for 24 h. (D) HEp-2 and A549 cells infected with RSV A2 (moi = 1) were treated or not (CV) with imiquimod (10 μg/ml) at 0, 2, 4, 6, 8, 12 and 16 h p.i. Total virus yields were determined by plaque assay in Vero cells at 24 h p.i and plotted as the percentage of inhibition with respect to untreated–infected control (CV). Data represent mean ± SD for n = 3 independent experiments, performed in duplicate. *Significantly different from CV (p-value < 0.05); One way ANOVA with Tukey post test.

no cytotoxic effect at all concentrations tested (CC_{50} > 50 μg/ml).

Next, we evaluated whether the antiviral action against RSV was due to a direct inactivation of the released virus. Suspensions of RSV A2 and line 19 were incubated with different concentrations of imiquimod for 120 min at 37 °C, followed by titration of the remaining infectivity in Vero cells. No reduction in viral titers was observed after treatment with imiquimod with respect to untreated control, suggesting that it did not exert a virucidal activity (Fig. 2B).

3.3. Influence of the duration of treatment with imiquimod on RSV infectivity

To further characterize imiquimod inhibitory action, HEp-2 and A549 cells were exposed to imiquimod before, during or after infection with RSV A2, and virus yields were quantified at 24 h p.i. When imiquimod was added before or during RSV inoculation (moi = 1), no significant inhibition of viral multiplication was detected. However, RSV A2 virus yields significantly decreased when imiquimod was added after infection in HEp-2 and A549 cells (Fig. 2C).

Then, we decided to make a time of addition assay at different times after infection. Results showed that imiquimod was able to inhibit infectious particle formation even when it was added at 8 h p.i. (Fig. 2D). At later times points, imiquimod inhibition of viral replication decreased in HEp-2 and A549 cells (Fig. 2D). Hence, considering that imiquimod restrained its antiviral activity even when it was added at 8 h p.i., it suggested that imiquimod did not affect an early step in the viral life cycle, such as viral entry.

3.4. Effect of imiquimod on virus macromolecular synthesis

One of the most important steps in virus multiplication cycle after entry into the host cell is the synthesis of viral RNA and proteins. Thus, first, we examined if viral RNA synthesis was affected by imiquimod in HEp-2 cells. For that purpose, intracellular RNA synthesis of RSV A2 was analyzed by qRT-PCR at different time points p.i. in the presence or absence of imiquimod (Fig. 3A). The amounts of viral RNA in untreated and treated cells were calculated in comparison to the content of viral RNA in untreated infected cells at 6 h p.i., defined as 1. At 6 h and 15 h p.i., the content of viral RNA in cells infected with RSV and treated with imiquimod was not statistically different to that in untreated infected cells. By contrast, the relative contents of viral RNA in cells infected and treated with imiquimod were significantly reduced in comparison to untreated infected cells at 24 h p.i., when the peak in RNA synthesis was detected for untreated cells (Fig. 3A). These results suggested that treatment with imiquimod impaired viral RNA synthesis during RSV infection.

Then, to evaluate the effect of imiquimod on the expression of RSV proteins, IF analyses was performed using an anti-glycoprotein F (gF)

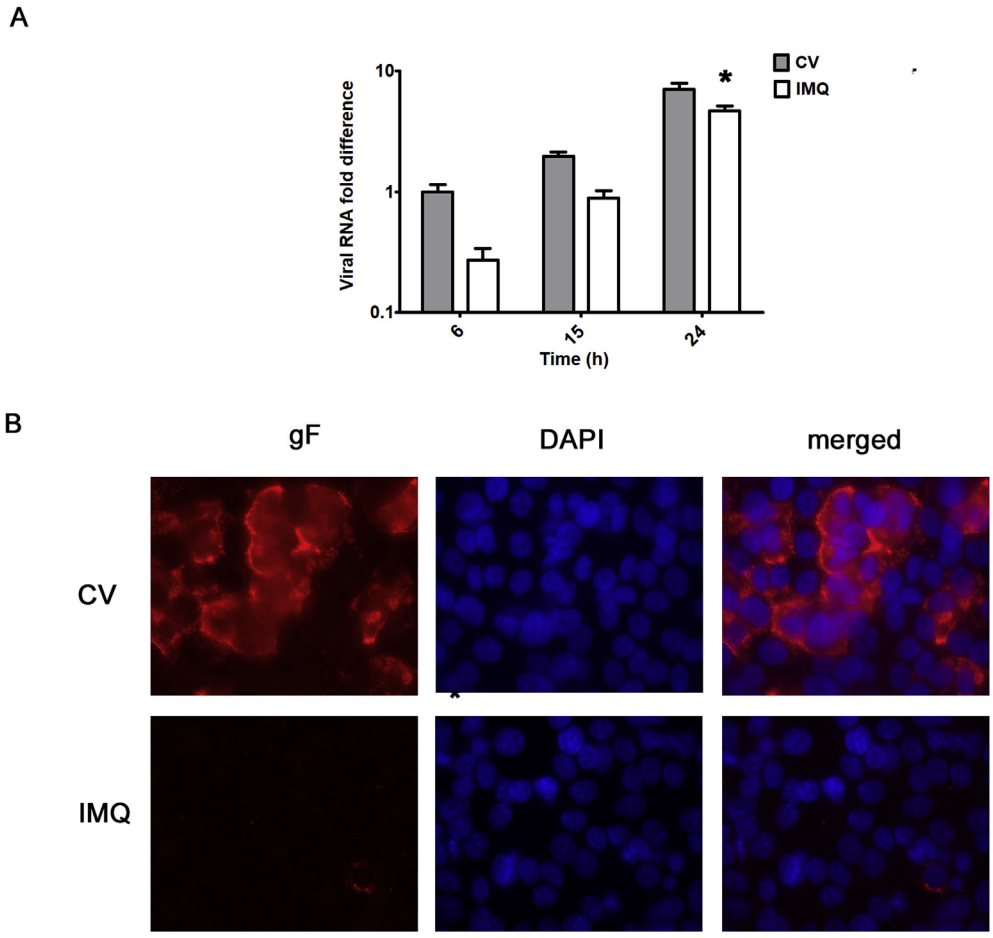

Fig. 3. Effect of imiquimod on virus macromolecular synthesis. (A) *Viral RNA synthesis*. Total cellular RNA was extracted at the indicated times p.i. and viral RNA was quantified by qRT-PCR. The amounts of viral RNA in untreated and treated with imiquimod (10 μg/ml) HEp-2 cells were calculated in comparison to the content of viral RNA in untreated infected cells at 6 h p.i., defined as 1. *Significantly different from CV (p-value < 0.05); two-way ANOVA with Bonferroni's post test. (B) *Protein expression*. IF staining was performed to detect the intracellular localization of gF in HEp-2 cells infected with RSV A2 and treated or not with imiquimod (10 μg/ml) at 24 h p.i. Magnification: 400X. Data represent mean ± SD for n = 3 independent experiments, performed in duplicate. *Significantly different from CV (p-value < 0.05); One way ANOVA with Tukey post test.

antibody (Fig. 3B). We found that the majority of untreated infected HEp-2 cells expressed gF protein (92%). On the other hand, a limited appearance of fewer and scattered foci expressing gF was observed when infected cells were treated with imiquimod, and the number of fluorescent cells expressing gF was reduced to 7% in HEp-2 infected cells treated with imiquimod (Fig. 3B).

Altogether, these results suggested that treatment with imiquimod affected the ability of RSV particles to drive the biosynthesis of viral macromolecules within the host cell. Even though imiquimod seemed to inhibit more effectively viral protein expression than viral RNA synthesis, the synthesis of both viral macromolecules were significantly affected by imiquimod, that could finally lead to the markedly decreased in the amounts of infectious virus particles observed in infected cells treated with imiquimod (Figs. 1 and 2A).

3.5. Antiviral activity of imiquimod was dependent on the PKA pathway

Although imiquimod is known as an agonist for TLR7, another TLR7 agonist, resiquimod, did not show anti-RSV activity in HEp-2 and A549 cells (Fig. 1). As expected from previous studies (Tissari et al., 2005; Han et al., 2014), both HEp-2 and A549 cells did not express a functional TLR7 receptor, since these TLR7 agonists neither induced cytokine production nor triggered activation of the transcription factor NF-κB following stimulation of HEp-2 and A549 cells (Supplementary Fig. 1). In contrast, poly (I:C)-HMW (TLR3 agonist) and Pam2CSK4 (TLR2/6 agonist) activated NF-κB and induced cytokine expression in these cells (Supplementary Fig. 1). Moreover, imiquimod demonstrated identical significant antiviral activity against RSV in HEp-2, A549 cells and in the type I interferon deficient Vero cell line (Table 1 and Fig. 2A). These results suggested that modulation of type I interferons and cytokines was not required for the protective effect of imiquimod. Thus, imiquimod transduced intracellular signals that elicit anti-RSV activity independently of an innate response. In this sense, Schön et al. (2006) reported that imiquimod acts not only as an agonist for TLR7 but also as an antagonist for adenosine receptors. Besides, Kan et al. (2012) demonstrated that imiquimod, but not resiquimod, inhibits HSV-1 replication via adenosine receptor A1/PKA pathway, independently of the TLR7 signaling pathway and IFN production. (Kan et al., 2012). Thus, we hypothesize that imiquimod might exert its anti-RSV activity through PKA pathway as well.

To test this suggestion, first we measured the effects of imiquimod in HEp-2 and A549 cells on CREB (cAMP response element-binding) phosphorylation, which is a known direct substrate of PKA (Naqvi et al., 2014). We found that imiquimod treatment increased the amount of p-CREB in total cell lysates, as early as 10 min (Fig. 4A). Interestingly, treatment with a selective PKA inhibitor (KT5720) significantly blocked imiquimod-induced phosphorylation of CREB (Fig. 4B), thereby providing additional evidence of PKA activation in imiquimod-treated epithelial cells. However, an adenosine receptor A1 agonist (R-PIA) did not affect imiquimod-induced CREB phoshorylation (Fig. 4B), suggesting that imiquimod might not be triggering CREB phoshorylation through adenosine receptor A1 in HEp-2 and A549 cells. Since KT5720 decreased the imiquimod-induced CREB phosphorylation, we sought to investigate whether KT5720 was able to attenuate the antiviral effect of imiquimod. In concordance with these results, imiquimod failed to inhibit RSV replication in HEp-2 and A549 cells treated with KT5720, whereas imiquimod conserved its antiviral activity in cells treated with R-PIA (Fig. 4C). Given the fact that imiquimod affected the ability of RSV particles to drive the biosynthesis of viral macromolecules, such as gF (Fig. 3B), we investigated whether KT5720 was able to reduce the

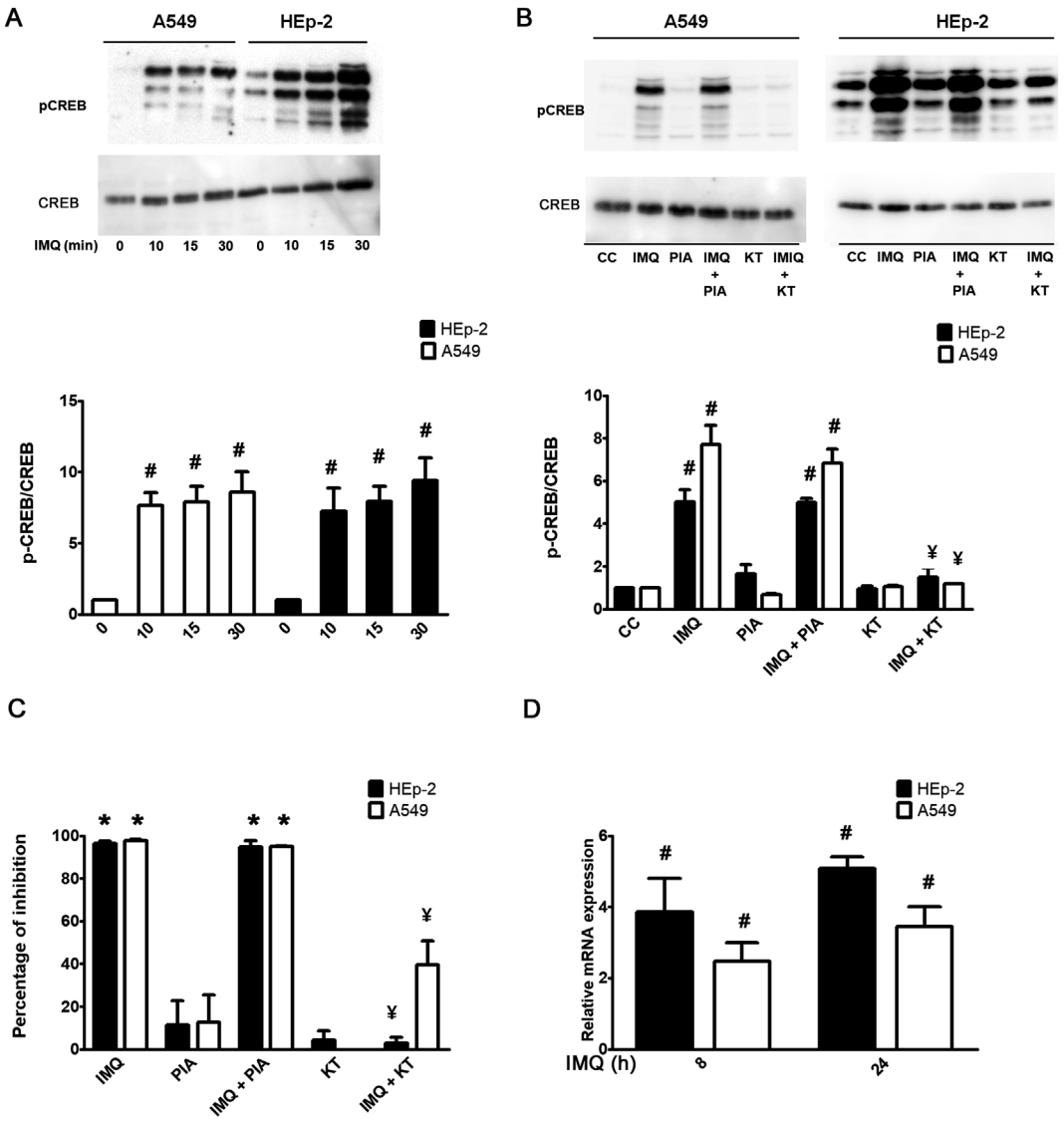

Fig. 4. Effect of imiquimod on the PKA pathway. (A) Immunoblot images of p-CREB and CREB expression, and quantitative densitometric analysis in HEp-2 and A549 epithelial cells after exposure to either vehicle or imiquimod (10 μg/ml) during the indicated times. (B) Immunoblot images of p-CREB and CREB expression, and quantitative densitometric analysis in HEp-2 and A549 cells after exposure or not to R-PIA (10 μM) or KT5720 (10 μM) pretreatment for 15 min, and then stimulated or not with imiquimod (10 μg/ml) for 10 min. (C) HEp-2 and A549 cells were treated or not with R-PIA (10 μM) or KT5720 (10 μM) for 15 min, and then infected with RSV A2 (moi = 1) and treated or not with imiquimod plus R-PIA or KT5720 for 24 h. Total virus yields were determined by plaque assay in Vero cells and plotted as the percentage of inhibition with respect to untreated–infected control (CV). (D) Expression of cystatin A in HEp-2 and A549 cells treated with imiquimod (10 μg/ml). At the indicated times after treatment, total RNA was extracted and gene expression was determined by real-time PCR. Data were analyzed using the $2^{-\Delta\Delta Ct}$ formula. Actin was used as an internal for determination of gene expression. (CC): cell control (unstimulated and uninfected cells). (CV): untreated–infected control cells. Data represent mean ± SD for n = 3 independent experiments, performed in duplicate. *Significantly different from CV (p-value < 0.05); # significantly different from CC (p-value < 0.05); ¥Significantly different from imiquimod treated cells (p-value < 0.05); One way ANOVA with Tukey post test. There were no statistically significant differences between imiquimod treated cells and imiquimod plus R-PIA treated cells regarding both p-CREB expression and virus yields.

inhibition of gF expression by imiquimod, as well. Interestingly, imiquimod did not decrease gF expression in HEp-2 cells treated with KT5720 (Supplementary Fig. 2). Moreover, taking into account that PKA is one of the major families of eukaryotic cyclic adenosine monophosphate (cAMP) receptors, and, therefore, it is activated by cAMP, we hypothesized that elevated intracellular cAMP might decrease RSV titers and gF expression. To test this possibility, HEp-2 cells were infected with RSV in the presence or absence of forskolin, a potent inductor of cAMP production, or the cAMP analog dibutyryl cAMP (dbcAMP), and viral titers and expression of gF were analyzed. We found that both viral titers and expression of gF significantly decreased in HEp-2 cells treated with either forskolin or dbcAMP (Supplementary Fig. 2). Thus, these results suggested that an increase in cAMP levels, wich in turn activates PKA, inhibited gF expression and attenuated viral replication in epithelial cells.

Considering that the anti-HSV-1 activity of imiquimod is closely related to cystatin A induction via PKA (Kan et al., 2012), the effect of imiquimod on the mRNA expression of cystatin A in HEp-2 and A549 cells was investigated. We found that cystatin A was significantly up-regulated by imiquimod treatment in HEp-2 and A549 cells (Fig. 4D).

Thus, these findings suggested that imiquimod might exert its anti-RSV activity in HEp-2 and A549 cells by activating PKA, and probably, through its downstream signaling effectors, such as cystatin A.

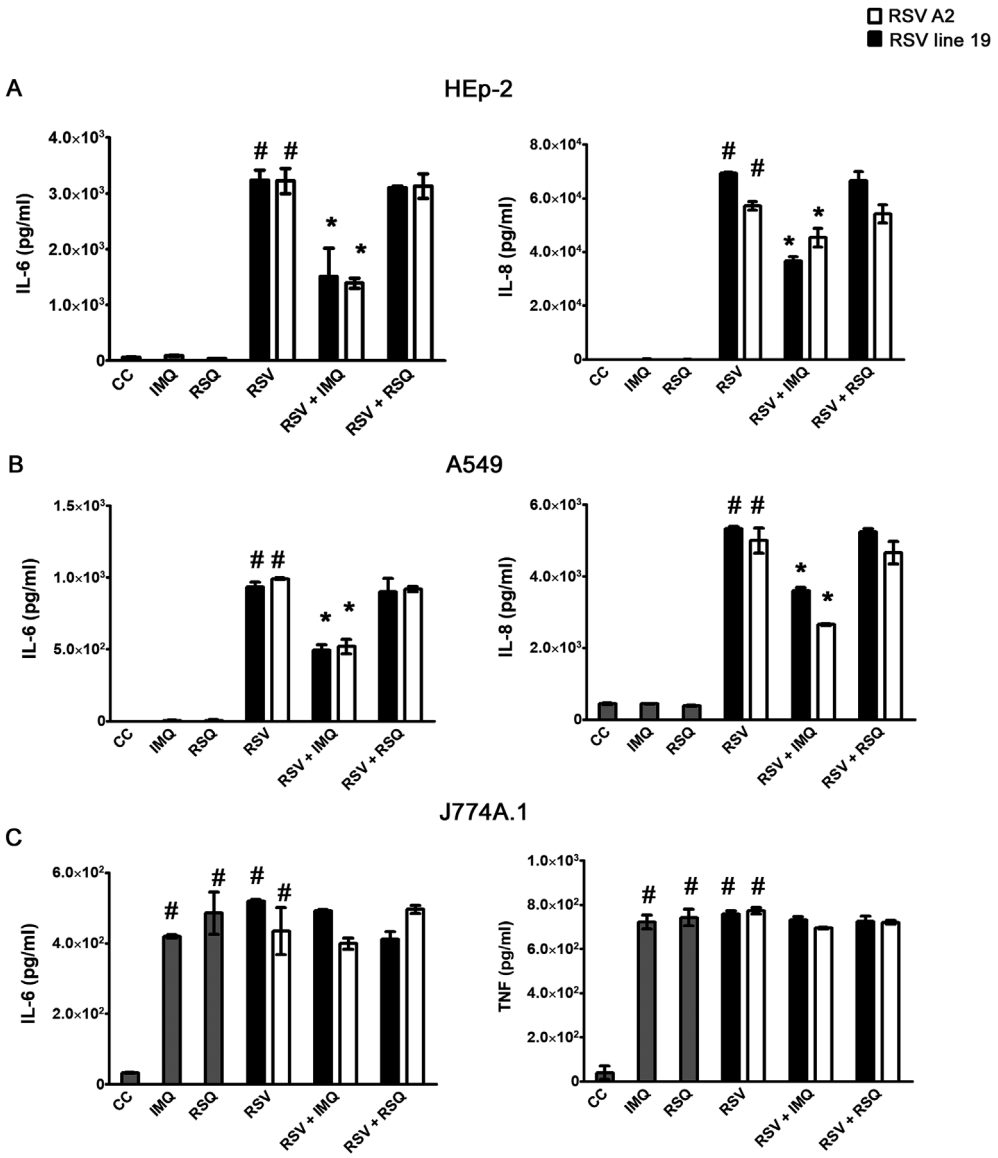

Fig. 5. Effect of imiquimod on cytokine production in RSV infected cells. HEp-2 (A), A549 (B) and J774A.1 (C) cells were infected with RSV A2 and line 19 (moi = 1) and treated or not with imiquimod (10 μg/ml) and resiquimod (10 μg/ml) during 24 h. IL-6, IL-8 and TNF-α was determined by ELISA. CC: cell control (unstimulated and uninfected cells). Data represent mean ± SD for n = 3 independent experiments, performed in triplicate. * Significantly different from RSV infected cells (p-value < 0.05). # Significantly different from CC (p-value < 0.05); One way ANOVA with Tukey post test.

3.6. Modulation of cytokine production by imiquimod in infected epithelial and macrophage cell lines

It has been already reported that RSV is able to induce the expression of pro-inflammatory cytokines including IL-6 and TNF-α and chemokines such as IL-8, that contribute to inflammation and the pathology of the infection (Masaki et al., 2011; Li et al., 2016; Salinas et al., 2019). Thus, we measured the effect of imiquimod on IL-6 and IL-8 secretion in infected epithelial cells, and IL-6 and TNF-α in infected macrophage cell line. As a control, cells were also treated with resiquimod. Supernatants harvested from HEp-2, A549 and J774A.1 cells infected with RSV A2 and line 19 strains (moi = 1) and treated or not with imiquimod (10 μg/ml) and resiquimod (10 μg/ml) were used to quantify IL-6, IL-8 and TNF-α by ELISA.

As expected from previous results (Supplementary Fig. 1), no significant differences between cytokines release from untreated and imiquimod and resiquimod-treated epithelial cells were detected. Besides, we found that imiquimod significantly decreased RSV-induced IL-8 and IL-6 expression in HEp-2 and A549 cells, whereas resiquimod did not affect cytokine production in RSV-infected HEp-2 and A549 cells (Fig. 5). In contrast, in J774A.1 cells, imiquimod and resiquimod stimulated pro-inflammatory cytokine secretion, and, interestingly, we observed that neither imiquimod nor resiquimod affected RSV induced-IL-6 and TNF-α production in these cells.

3.7. In vivo evaluation of imiquimod antiviral effect

Having demonstrated that imiquimod had antiviral and immunomodulatory properties against RSV A2 and line 19 *in vitro*, the question whether these properties were functional *in vivo* was addressed. For that purpose, a well-characterized model of murine pulmonary RSV infection was used (Lukacs et al., 2006; Stokes et al., 2011; Woolums et al., 2011; Rudd et al., 2016; Salinas et al., 2019). In uninfected mice, an i.n. dose of 5 mg/kg of imiquimod had no effect on general health and behavior. Thus, 1 h after RSV A2 and line 19 infection by nasal instillation, mice were treated with i.n. administration of 5 mg/kg of imiquimod. Then, mice were subsequently treated with daily administration with imiquimod until day 4 p.i. Mice inoculated

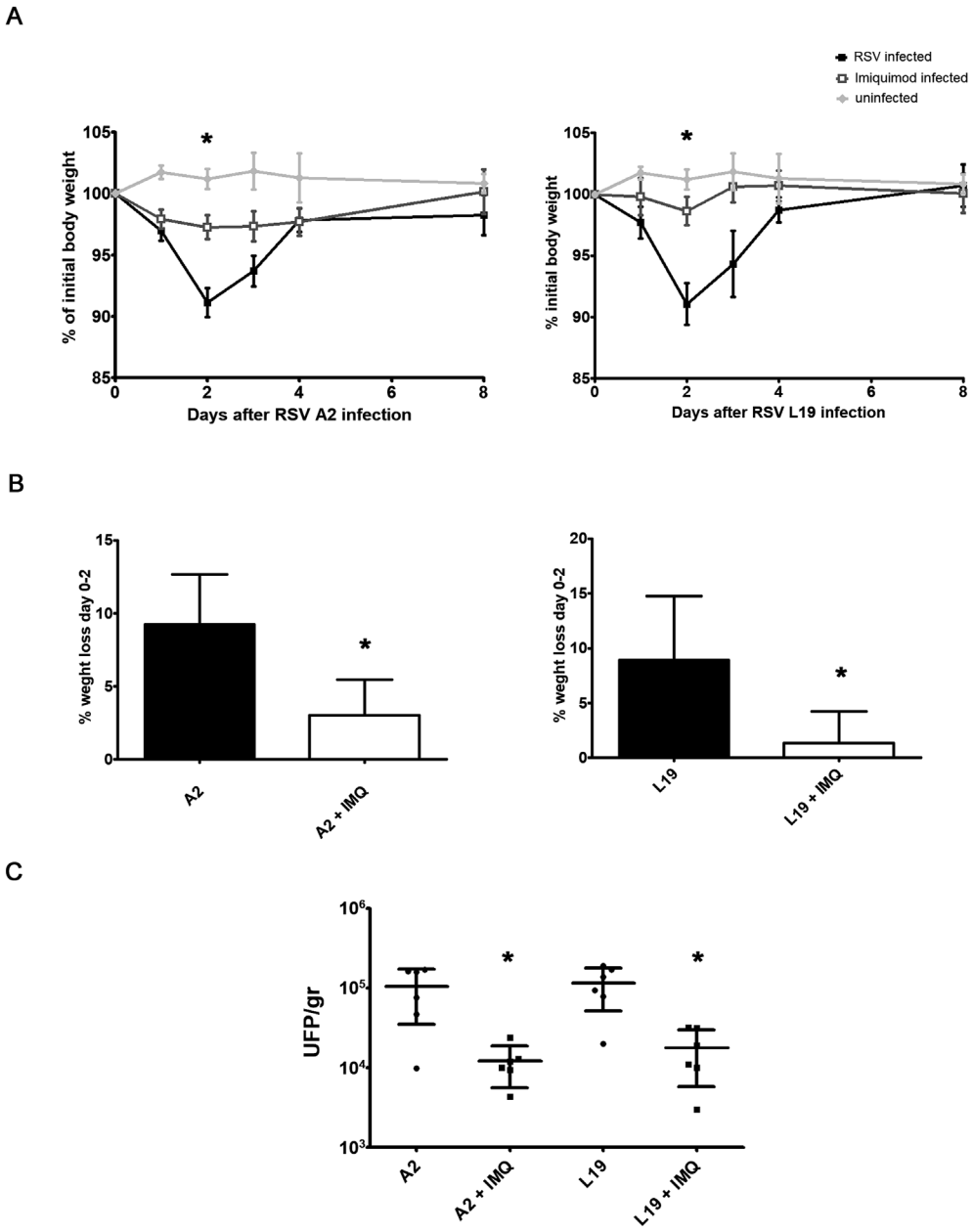

Fig. 6. *In vivo* evaluation of imiquimod antiviral effect. Female Balb/c mice were infected with RSV line 19 and A2 (5×10^6 PFU) by intranasal (i.n.) instillation, concomitant with 5 mg/kg of imiquimod by i.n. administration on day 0. On days 1–4, all mice received further inoculations of imiquimod i.n. (A–B) Weight was monitored and assessed as a percentage of starting weight. Day 0 refers to time right before inoculation. * at day 2, values for imiquimod-treated infected mice were significantly higher than infected mice (p-value < 0.05). (C) The animals were killed on day 4 and the lungs were used for titration of infectious virus. Data show mean ± SD from n = 6 mice/condition. *Significantly different from RSV infected mice (p-value < 0.05); One way ANOVA with Tukey post test.

i.n. with PBS were used as untreated controls. Weight loss was assessed daily, viral load was determined on day 4 p.i. (the time point of peak viral load in this model), and pulmonary gene transcription and histopathology was assessed on day 8, given that the pathology is most severe between days 5 and 8 p.i., when peaks the progression of peribronchovascular infiltrates and inflammation (Stokes et al., 2011; Rudd et al., 2016).

Weight loss is a quantitative measure of RSV illness severity in the BALB/c mouse model (Stokes et al., 2011; Rudd et al., 2016). A2 and Line 19 RSV-infected mice showed an early weight reduction on day 2 p.i., (Fig. 6A and B) (Stokes et al., 2011; Rudd et al., 2016; Salinas et al., 2019). In contrast, RSV A2 and line 19 infected mice treated with imiquimod not only had significantly less weight loss on day 2 p.i., but also over the entire course of the experiment when compared to untreated infected controls (Fig. 6A and B). In concordance with that, RSV A2 and line 19 titers in the lung were significantly lower in imiquimod-treated mice compared to untreated animals at day 4 (Fig. 6C).

A number of cytokines have previously been outlined to be important in the severity of the pathophysiology and the induction of AHR and mucus (Woolums et al., 2011). Previously, it was shown that RSV A2 and line 19 infected mice induce the transcription of pro-inflammatory cytokines TNF-α and IL-6, Th2-type cytokine IL-4, Th1-type cytokine IFN-γ, and Th17-type cytokine IL-17 A, in the lungs with respect to uninfected animals (Salinas et al., 2019). Interestingly, infected mice treated with imiquimod had significantly lower levels of all these cytokines than those observed in control infected animals (Fig. 7).

As shown in Fig. 8, RSV A2 and line 19 infections recapitulated previously reported abnormal histology of lung sections (Rudd et al., 2016). H&E staining showed alveolar walls, and alveolar spaces filled with moderate to severe inflammatory infiltrates of cells in infected and mock-treated group. The lung sections from imiquimod treated group were more closely resembled to that of the uninfected controls (Fig. 8A). In concordance, results of semiquantitative histological scoring showed that imiquimod significantly reduced RSV-induced pathological changes (Fig. 8B). Thus, imiquimod reduced lung inflammation and inflammatory cell infiltration (Fig. 8).

Taken together, these results, demonstrated that imiquimod restrained RSV infection in the lung, as well as modulated cytokine

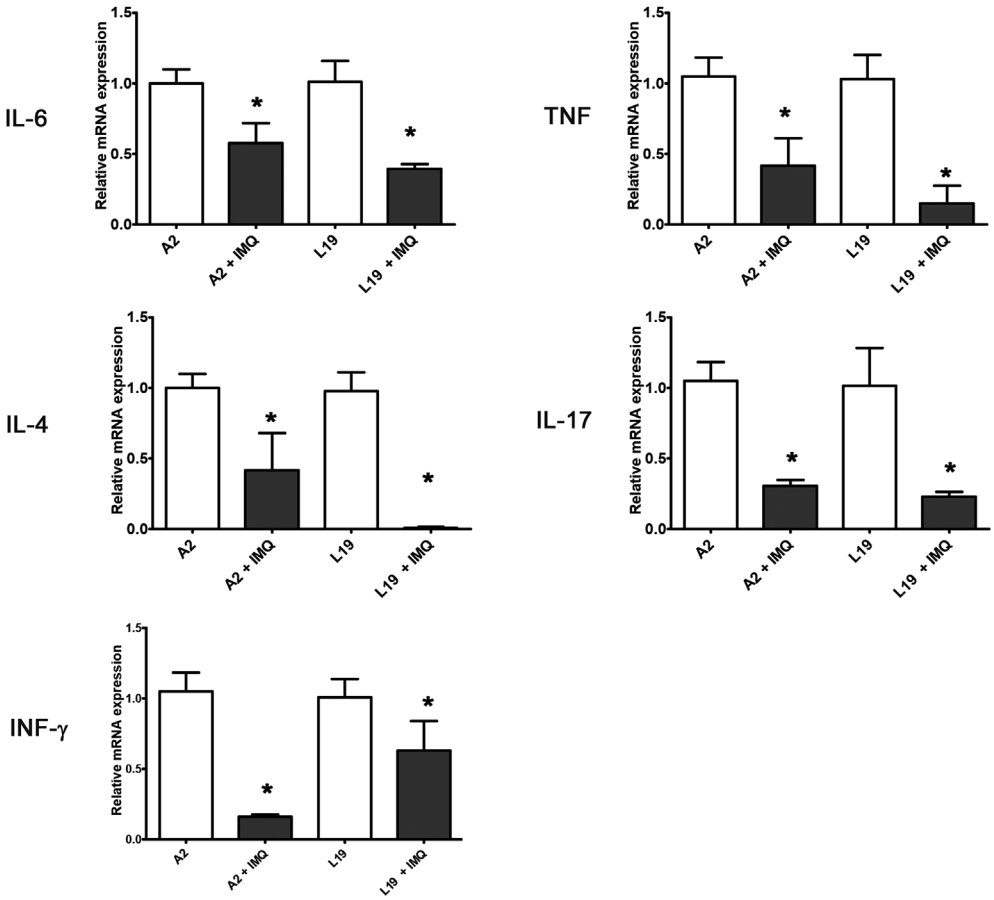

Fig. 7. Cytokines gene expression determined by real-time PCR. Pulmonary cytokines expression was assessed on day 8 p.i. and the data were analyzed using the $2^{-\Delta\Delta Ct}$ formula. Actin was used as an internal for determination of gene expression. Data show mean ± SD from n = 3 mice/condition. *Significantly different from RSV infected mice (p-value < 0.05); One way ANOVA with Tukey post test.

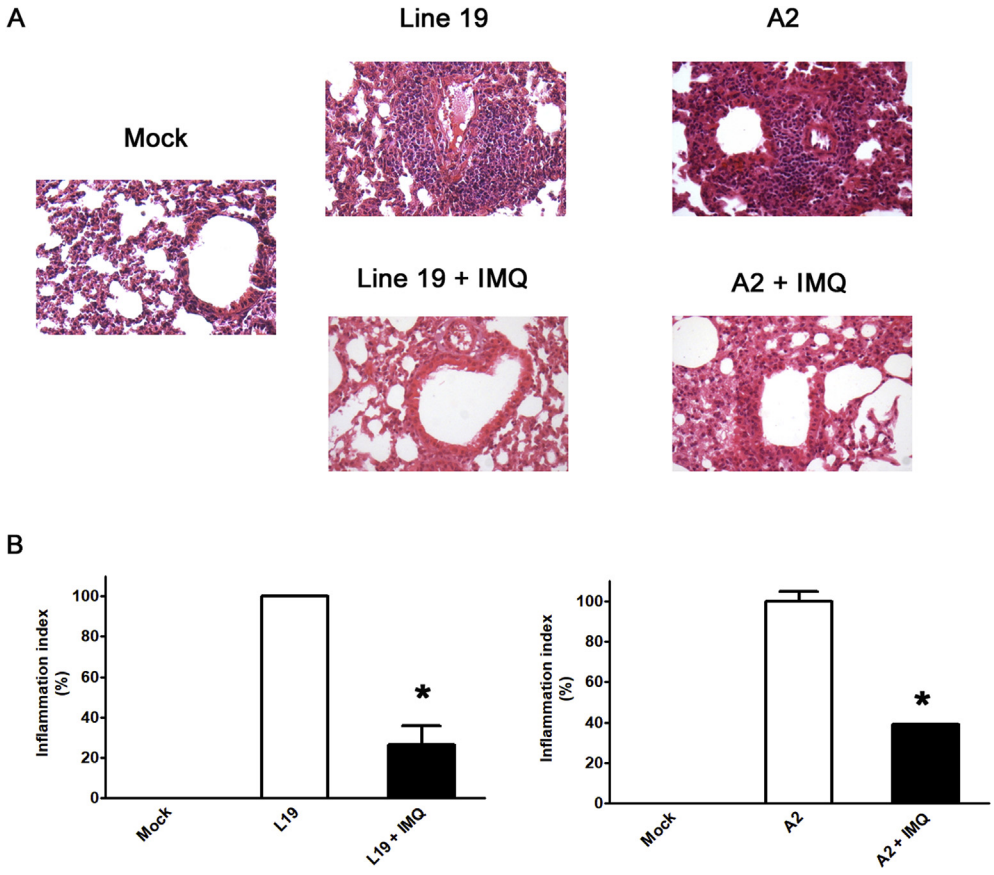

Fig. 8. Lung histology. (A) Light micrographic images of pulmonary histology of H &E-stained lungs collected at day 8 p.i., shown at original magnification x100, representative of n = 3/condition. (B) An index of pathologic changes in H&E slides was obtained by scoring the inflammatory infiltrate around the airways and vessels for greatest severity. The Inflammation Index was calculated as the average of the airways' index, and it was plotted as percentage with respect to mock-treated infected mice, which was considered 100% of inflammation. *Significantly different from mock-treated infected mice (p-value < 0.05); One way ANOVA with Tukey post test.

response and ameliorated lung injury.

4. Discussion

Imiquimod is known as a TLR7 agonist, but additionally acts as an antagonist for adenosine receptors (Schön et al., 2006). Currently, it is used in the treatment of human papilloma virus genital warts (Schön and Schön, 2006). Besides, it has direct antiviral activity against HSV-1 in human amnion cells, and moreover, it decreases total intracellular HBV DNA as well as secretion of HBe antigens in hepatocytes, *in vitro,* independently of the TLR signaling pathway (Kan et al., 2012; Lucifora et al., 2018).

In this study, we found anti-RSV activity of imiquimod, but not resiquimod, in HEp-2 and A549 cells, and this phenotype is independent of an innate response. Interestingly, although Pam2CSK4 and poly(I:C)-HMW activate the innate response in A549 and HEp-2 cells, we do not observe anti-RSV activity of these TLR ligands. In this sense, there is compelling evidence that RSV is able to interfere with TLR signaling pathways. For instance, it has been reported that RSV interferes with TLR7 and TLR9 signaling pathways in human plasmacytoid dendritic cells, and with TLR3 and TLR9 in mice (Guerrero-Plata et al., 2005; Schlender et al., 2005). Thus, RSV may interfere with the activation of the innate response induced by TLR2/6 and TLR3 ligands in HEp-2 and A549 cells.

Herein, we identified PKA as a key downstream effector of imiquimod actions against RSV in HEp-2 and A549 cells, similarly as it was shown for HSV-1 (Kan et al., 2012). This conclusion is based on biochemical evidence of PKA activation (phosphorylation of CREB) in imiquimod-treated epithelial cells. Additionally, PKA inhibition by KT5720 blocks imiquimod-induced phosphorylation of CREB, and importantly, imiquimod antiviral effects and imiquimod inhibition of gF expression, as well. Considering that R-PIA, a selective A1 adenosine agonist, does not affect imiquimod-induced phosphorylation of CREB and imiquimod antiviral activity under our treatment conditions, we cannot exclude the possibility that imiquimod may act as an inverse agonist of another G-protein-coupled receptor (GPCR) coupled to Gαi, or as an agonist of a GPCR coupled to Gαs, present in these cells.

PKA is one of the major families of eukaryotic cAMP receptors together with the exchange protein directly activated by cAMP (EPAC) (Cheng et al., 2008). The development of inhibitors specific to cAMP, PKA and EPAC has enabled researchers to study the importance of this signaling under various cellular conditions, including viral infection (Rezaee et al., 2017; Choi et al., 2018). In this sense, as well as the reported anti-HSV-1 activity of imiquimod as a consequence of its activation of cAMP/PKA (Kan et al., 2012), there are other recent studies on the potential effect of cAMP/PKA and cAMP/EPAC activators or inhibitors on viral replication. For instance, activation of either cAMP/PKA or EPAC/Rap1-dependent signaling has been shown to inhibit HIV-1 replication and cell-to-cell HIV-1 transfer (Hayes et al., 2002; Clemente et al., 2014). On the other hand, selective inhibition of EPAC significantly reduced susceptibility to Middle East respiratory syndrome coronavirus (MERS-CoV) infections (Tao et al., 2014). Particularly in case of RSV infections, inhibition of cellular EPAC2 protein significantly prevents RSV replication and RSV-induced inflammatory responses *in vitro* (Choi et al., 2018). Moreover, Rezaee et al. (2017) found that the activation of the cAMP/PKA signaling pathway by forskolin and a stable cell-permeable analog of cAMP attenuate RSV-induced disruption of structure and functions of the airway epithelial barrier and, besides, inhibit expression of RSV A2 F mRNA *in vitro*. Similarly, we have observed that forskolin and an analog of cAMP reduce the amounts of infectious viral particles and affect gF expression in epithelial cells (Supplementary Fig. 2). Taken together, our present study and the described publications highlight cAMP/PKA and cAMP/EPAC pathways as potent modulators of viral infections *in vitro*, suggesting they could be a promising therapeutic target for viral infections *in vivo*.

Airway epithelial cells are the major target of RSV infection in the lung, and we have shown that imiquimod has concentration-dependent antiviral activity against RSV strains A2 and line 19 in epithelial cells when added after infection. Besides, imiquimod essentially restricts RSV infection after viral entry into the host cell, interfering with viral RNA and protein synthesis. Likewise, Kan et al. (2012) reported that imiquimod suppresses HSV-1 replication without affecting HSV-1 entry.

Despite the valuable information that infected cells and tissues may provide, animal models are essential to analyze the safety, efficacy and mechanisms of antiviral and immunomodulatory compounds in the complex physiology of the lungs. Notably, in this study we have verified that there is a reduction of the viral titers in the lungs in mice infected with RSV A2 and line 19 treated with imiquimod. This is particularly important, as some studies have shown that virus-induced pathogenesis and disease severity are positively correlated with viral load (Buckingham et al., 2000; DeVincenzo et al., 2010; Houben et al., 2010; Torres et al., 2010; De Clercq, 2015; Skjerven et al., 2016). In this sense, imiquimod not only exerts a reduction of the viral titers in the lung, but also a decrease in weight loss and airway inflammation. Interestingly, we also found that imiquimod is able to reduce pro-inflammatory cytokines production in human epithelial cells infected with RSV. Importantly, RSV productively multiplies in these cell lines. However, RSV does not multiply in J774A.1 cells in our experimental settings, and strikingly, imiquimod did not reduce cytokine production in this cell line. Thus, considering these findings, and that the induction of many proinflammatory mediators is virus replication dependent in epithelial cells, we speculate that imiquimod might not directly modulate cytokine production in infected cells, and it probably affects cytokine/chemokine induction in epithelial cells solely as a consequence of its control of viral replication *in vitro*. Likewise, we hypothesize that the beneficial effect of imiquimod on airway and lung inflammation could be mainly an indirect consequence of imiquimod-suppressed RSV replication. Similarly, it is proposed that imiquimod is able to reduce pulmonary inflammation and weight loss following influenza A virus infection because of its capacity to clear virus during the acute infection phase of infection (To et al., 2019). However, it was previously reported that the immune response to RSV infection in TLR7−/− mice is more pathogenic compared to wild-type mice, associated with an alteration in T cell and dendritic cell responses (Lukacs et al., 2010). Thus, considering the central role of the TLR7 signaling in the immune response against RSV infection, we cannot exclude the possibility that imiquimod may attenuate the airway inflammation through direct modulation of the immune response via TLR7 signaling as well.

Overall, given that viral replication and lung inflammation are key risk factors for RSV disease severity, imiquimod inhibitory effect on both the production of infectious progeny viruses and airway inflammation in mice, supports imiquimod as a promising therapeutic alternative to control RSV replication and pathogenesis. Interestingly, it has been recently reported that intranasal delivery of imiquimod results in a reduction in viral replication, bodyweight loss and airway inflammation following influenza A virus infection (To et al., 2019). Thus, these findings together with and our results support imiquimod as a strong candidate for the treatment of respiratory viral infections. In order to analyze whether imiquimod restrains RSV infection solely via PKA pathway *in vivo*, further specific activators and/or inhibitors involved in this pathway should be examined in animals infected with RSV.

5. Conclusion

This study demonstrates that imiquimod has direct antiviral activity against RSV via PKA pathway, and, probably as a consequence of these anti-RSV properties, imiquimod displays cytokine modulating activity in RSV infected cells, *in vitro*. Moreover, in a murine model of RSV infection, imiquimod treatment improves the course of acute disease, evidenced by decreased weight loss, reduced RSV lung titers, and attenuated airway inflammation. Consequently, imiquimod represents a

promising therapeutic alternative against RSV infection and may inform the development of novel therapeutic targets to control RSV pathogenesis.

Declaration of competing interest

None.

Acknowledgements

We thank Guillermo Assad Ferek for their technical assistance. We thank Dr. Laura Talarico (INFANT–Buenos Aires, Argentina) for providing RSV strains A2 and line 19. The authors are deeply grateful to the staff of the UOCCB, ANLIS-Malbrán, Buenos Aires, for their expert technical assistance in the ABSL-3 laboratory. This work was supported by Grants from ANPCyT (PICT Nº 2016–1821, 2014-3331 and PICT 2013-2281), CONICET (PIP 20120100538) and UBA (20020130100584BA and 20020170100175BA).

Appendix A. Supplementary data

Supplementary data to this article can be found online at https://doi.org/10.1016/j.antiviral.2020.104817.

References

Boivin, N., Sergerie, Y., Rivest, S., Boivin, G., 2008. Effect of pretreatment with toll like receptor agonists in a mouse model of herpes simplex virus type 1 encephalitis. J. Infect. Dis. 198 (5), 664–672.

Borchers, A.T., Chang, C., Gershwin, M.E., Gershwin, L.J., 2013. Respiratory syncytial virus–a comprehensive review. Clin. Rev. Allergy Immunol. 45, 331–379.

Boukhvalova, M.S., Sotomayor, T.B., Point, R.C., Pletneva, L.M., Prince, G.A., Blanco, J.C., 2010. Activation of interferon response through toll-like receptor 3 impacts viral pathogenesis and pulmonary toll-like receptor expression during respiratory syncytial virus and influenza infections in the cotton rat Sigmodon hispidus model. J. Interferon Cytokine Res. 30 (4), 229–242. https://doi.org/10.1089/jir.2009.0025.

Buckingham, S.C., Bush, A.J., Devincenzo, J.P., 2000. Nasal quantity of respiratory syncytical virus correlates with disease severity in hospitalized infants. Pediatr. Infect. Dis. J. 19 (2), 113 ± 7.

Bueno, C.A., Michelini, F.M., Pertino, M.W., Gómez, C.A., Schmeda-Hirschmann, G., Alché, L.E., 2015. Natural and semisynthetic diterpenoids with antiviral and immunomodulatory activities block the ERK signaling pathway. Med. Microbiol. Immunol. 204 (5), 575–584.

Cheng, X., Ji, Z., Tsalkova, T., Mei, F., 2008. Epac and PKA: a tale of two intracellular cAMP receptors. Acta Biochim. Biophys. Sin. 40 (7), 651 ± 62.

Choi, E.J., Ren, Y., Chen, Y., Liu, S., Wu, W., Ren, J., Wang, P., Garofalo, R.P., Zhou, J., Bao, X., 2018. Exchange proteins directly activated by cAMP and their roles in respiratory syncytial virus infection. J. Virol. 29 (22), 92. https://doi.org/10.1128/JVI.01200-18. pii: e01200-18.

Clemente, M.I., Alvarez, S., Serramia, M.J., Martinez-Bonet, M., Munoz-Fernandez, M.A., 2014. Prostaglandin E2reduces the release and infectivity of new cell-free virions and cell-to-cell HIV-1 transfer. PloS One 9 (2), e85230. https://doi.org/10.1371/journal.pone.0085230.

De Clercq, E., 2015. Chemotherapy of respiratory syncytial virus infections: the final breakthrough. Int. J. Antimicrob. Agents 45 (3), 234–237.

DeVincenzo, J.P., Wilkinson, T., Vaishnaw, A., Cehelsky, J., Meyers, R., Nochur, S., 2010. Viral load drives disease in humans experimentally infected with respiratory syncytial virus. Am. J. Respir. Crit. Care Med. 182 (10), 1305 ± 14.

Guerrero-Plata, A., Baron, S., Poast, J.S., Adegboyega, P.A., Casola, A., Garofalo, R.P., 2005. Activity and regulation of alpha interferon in respiratory syncytial virus and human metapneumovirus experimental infections. J. Virol. 79 (16), 10190–10199.

Han, Y., Bo, Z.J., Xu, M.Y., Sun, N., Liu, D.H., 2014. The protective role of TLR3 and TLR9 ligands in human pharyngeal epithelial cells infected with influenza A virus. KOREAN J. PHYSIOL. PHARMACOL. 18 (3), 225–231. https://doi.org/10.4196/kjpp.2014.18.3.225.

Hayes, M.M., Lane, B.R., King, S.R., Markovitz, D.M., Coffey, M.J., 2002. Prostaglandin E (2) inhibits replication of HIV-1 in macrophages through activation of protein kinase A. Cell. Immunol. 215 (1), 61 ± 71.

Houben, M.L., Coenjaerts, F.E., Rossen, J.W., Belderbos, M.E., Hofland, R.W., Kimpen, J.L., Bont, L., 2010. Disease severity and viral load are correlated in infants with primary respiratory syncytial virus infection in the community. J. Med. Virol. 82, 1266–1271.

Kan, Y., Okabayashi, T., Yokota, S., Yamamoto, S., Fujii, N., Yamashita, T., 2012. Imiquimod suppresses propagation of herpes simplex virus 1 by upregulation of cystatin A via the adenosine receptor A1 pathway. J. Virol. 86 (19), 10338–10346. https://doi.org/10.1128/JVI.01196-12.

Kim, C., Ahmed, J.A., Eidex, R.B., Nyoka, R., Waiboci, L.W., Erdman, D., 2011. Comparison of nasopharyngeal and oropharyngeal swabs for the diagnosis of eight respiratory viruses by real-time reverse transcription- PCR assays. PloS One 6 (6), e21610 2011 Jun 30.

Kwon, Y.S., Park, S.H., Kim, M.A., Kim, H.J., Park, J.S., Lee, M.Y., Lee, C.W., Dauti, S., Choi, W.I., 2017. Risk of mortality associated with respiratory syncytial virus and influenza infection in adults. BMC Infect. Dis. (1), 785. https://doi.org/10.1186/s12879-017-2897-4.

Lanford, Robert, Guerra, Bernadette, Chavez, Deborah, Giavedoni, Luis, Hodara, Vida, Brasky, Kathleen, Fosdick, Abigail, Frey, Christian, Zheng, Jim, Wolfgang, Grushenka, Halcomb, Randall, Tumas, Daniel, 2013. GS-9620, an Oral Agonist of Toll-like receptor-7, Induces Prolonged Suppression of Hepatitis B Virus in Chronically Infected Chimpanzees. Gastroenterology 7 (144), 1508–1517. https://doi.org/10.1053/j.gastro.2013.02.003. In this issue.

Li, X.M., Sun, S.Z., Wu, F.L., Shi, T., Fan, H.J., Li, D.Z., 2016. Study on JNK/AP-1 signalling pathway of airway mucus hypersecretion of severe pneumonia under RSV infection. Eur. Rev. Med. Pharmacol. Sci. 20 (5), 853–857.

Lucifora, J., Bonnin, M., Aillot, L., Fusil, F., Maadadi, S., Dimier, L., Michelet, M., Floriot, O., Ollivier, A., Rivoire, M., Ait-Goughoulte, M., Daffis, S., Fletcher, S.P., Salvetti, A., Cosset, F.L., Zoulim, F., Durantel, D., 2018. Direct antiviral properties of TLR ligands against HBV replication in immune-competent hepatocytes. Sci. Rep. 29 (1), 5390. https://doi.org/10.1038/s41598-018-23525-w. 8.

Lukacs, N.W., Moore, M.L., Rudd, B.D., Berlin, A.A., Collins, R.D., Olson, S.J., Ho, S.B., Peebles Jr., R.S., 2006. Differential immune responses and pulmonary pathophysiology are induced by two different strains of respiratory syncytial virus. Am. J. Pathol. 169 (3), 977–986.

Lukacs, N.W., Smit, J., Nunez, G., Lindell, D., 2010. Respiratory Virus-induced TLR7 activation controls IL-17 associated Increase in mucus via IL-23 regulation. J. Immunol. 185 (4), 2231–2239.

Masaki, T., Kojima, T., Okabayashi, T., Ogasawara, N., Ohkuni, T., Obata, K., Takasawa, A., Murata, M., Tanaka, S., Hirakawa, S., Fuchimoto, J., Ninomiya, T., Fujii, N., Tsutsumi, H., Himi, T., Sawada, N., 2011. A nuclear factor-κB signaling pathway via protein kinase C δ regulates replication of respiratory syncytial virus in polarized normal human nasal epithelial cells. Mol. Biol. Cell 1 (13), 2144–2156 22.

Nair, H., Nokes, D.J., Gessner, B.D., Dherani, M., Madhi, S.A., Singleton, R.J., O'Brien, K.L., Roca, A., Wright, P.F., Bruce, N., Chandran, A., Theodoratou, E., Sutanto, A., Sedyaningsih, E.R., Ngama, M., Munywoki, P.K., Kartasasmita, C., Simões, E.A., Rudan, I., Weber, M.W., Campbell, H., 2010. Global burden of acute lower respiratory infections due to respiratory syncytial virus in young children: a systematic review and meta-analysis. Lancet 375 (9725), 1545–1555. https://doi.org/10.1016/S0140-6736(10)60206-1.

Naqvi, S., Martin, K.J., Arthur, J.S., 2014. CREB phosphorylation at Ser133 regulates transcription via distinct mechanisms downstream of cAMP and MAPK signalling. Biochem. J. 458 (3), 469 ± 79. https://doi.org/10.1042/BJ20131115.

Rezaee, F., Harford, T.J., Linfield, D.T., Altawallbeh, G., Midura, R.J., Ivanov, A.I., Piedimonte, G., 2017. cAMP-dependent activation of protein kinase A attenuates respiratory syncytial virus-induced human airway epithelial barrier disruption. PloS One 31 (12), e0181876. https://doi.org/10.1371/journal.pone.0181876.eCollection.2017. 7.

Rudd, P.A., Chen, W., Mahalingam, S., 2016. Mouse and cotton rat models of human respiratory syncytial virus. Methods Mol. Biol. 1442, 209–217. https://doi.org/10.1007/978-1-4939-3687-8_15.

Salinas, F.M., Vázquez, L., Gentilini, M.V., O Donohoe, A., Regueira, E., Nabaes Jodar, M.S., Viegas, M., Michelini, F.M., Hermida, G., Alché, L.E., Bueno, C.A., 2019. *Aesculus hippocastanum* L. seed extract shows virucidal and antiviral activities against respiratory syncytial virus (RSV) and reduces lung inflammation in vivo. Antivir. Res. 164, 1–11. https://doi.org/10.1016/j.antiviral.2019.01.018.

Sariol, C.A., Martinez, M.I., Rivera, F., Rodriguez, I.V., Pantoja, P., Abel, K., Arana, T., Giavedoni, L., Hodara, V., White, L.J., 2011. Decreased dengue replication and an increased anti-viral humoral response with the use of combined Toll-like receptor 3 and 7/8 agonists in macaques. PloS One 6 (4), e19323 2011.

Schlender, J., Hornung, V., Finke, S., Gunthner-Biller, M., Marozin, S., Brzozka, K., Moghim, S., Endres, S., Hartmann, G., Conzelmann, K.K., 2005. Inhibition of toll-like receptor 7- and 9-mediated alpha/beta interferon production in human plasmacytoid dendritic cells by respiratory syncytial virus and measles virus. J. Virol. 79, 5507–5515.

Schön, M.P., Schön, M., Klotz, K.N., 2006. The small antitumoral immune response modifier imiquimod interacts with adenosine receptor signaling in a TLR7- and TLR8-independent fashion. J. Invest. Dermatol. 126 (6), 1338–1347.

Schön, M.P., Schön, M., 2006. The small-molecule immune response modifier imiquimod: its mode of action and clinical use in the treatment of skin cancer. Expert Opin. Ther. Targets 10, 69–76.

Shinya, K., Okamura, T., Sueta, S., Kasai, N., Tanaka, M., Ginting, T.E., Makino, A., Eisfeld, A.J., Kawaoka, Y., 2011. Toll-like receptor pre-stimulation protects mice against lethal infection with highly pathogenic influenza viruses. Virol. J. 4 (8), 97. https://doi.org/10.1186/1743-422X-8-97.

Skjerven, H.O., Megremis, S., Papadopoulos, N.G., Mowinckel, P., Carlsen, K.H., Lodrup Carlsen, K.C., 2016. Virus type and genomic load in acute bronchiolitis: severity and treatment response with inhaled adrenaline. J. Infect. Dis. 13 (6), 915–921.

Smyth, R.L., Openshaw, P.J., 2006. Bronchiolitis. Lancet 368, 312–322.

Stokes, K.L., Chi, M.H., Sakamoto, K., Newcomb, D.C., Currier, M.G., Huckabee, M.M., Lee, S., Goleniewska, K., Pretto, C., Williams, J.V., Hotard, A., Sherrill, T.P., Peebles Jr., R.S., Moore, M.L., 2011. Differential pathogenesis of respiratory syncytial virus clinical isolates in BALB/c mice. J. Virol. 85 (12), 5782–5793. https://doi.org/10.1128/JVI.01693-10.

Tao, X., Mei, F., Agrawal, A., Peters, C.J., Ksiazek, T.G., Cheng, X., 2014. Blocking of exchange proteins directly activated by cAMP leads to reduced replication of Middle

East respiratory syndrome coronavirus. J. Virol. 88 (7), 3902 ± 10.
Tissari, J., Sirén, J., Meri, S., Julkunen, I., Matikainen, S., 2005. IFN-alpha enhances TLR3-mediated antiviral cytokine expression in human endothelial and epithelial cells by up-regulating TLR3 expression. J. Immunol. 174 (7), 4289–4294.
To, E.E., Erlich, J., Liong, F., Luong, R., Liong, S., Bozinovski, S., Seow, H.J., O'Leary, J.J., Brooks, D.A., Vlahos, R., Selemidis, S., 2019. Intranasal and epicutaneous administration of Toll-like receptor 7 (TLR7) agonists provides protection against influenza A virus-induced morbidity in mice. Sci. Rep. 9 (1), 2366. https://doi.org/10.1038/s41598-019-38864-5. 20.
Torres, J.P., Gomez, A.M., Khokhar, S., Bhoj, V.G., Tagliabue, C., Chang, M.L., 2010. Respiratory syncytial virus (RSV) RNA loads in peripheral blood correlates with disease severity in mice. Respir. Res. 11, 125.
Tregoning, J.S., Schwarze, J., 2010. Respiratory viral infections in infants: causes, clinical symptoms, virology, and immunology. Clin. Microbiol. Rev. 23, 74–98.
Turner, T.L., Kopp, B.T., Paul, G., Landgrave, L.C., Hayes Jr., D., Thompson, R., 2014. Respiratory syncytial virus: current and emerging treatment options. Clin. Outcomes Res. 25 (6), 217–225. https://doi.org/10.2147/CEOR.S60710.
Tuvim, M., Gilbert, B.E., Dickey, B.F., Evans, S.E., 2012. Synergistic TLR2/6 and TLR9 activation protects mice against lethal influenza pneumonia. PloS One 7 (1), e30596. https://doi.org/10.1371/journal.pone.0030596. Epub 2012 Jan 27.
Uematsu, S., Akira, S., 2006. Toll-like receptors and innate immunity. J. Mol. Med. (Berl.) 84 (9), 712–725.
Woolums, A., Lee, S., Moore, M., 2011. Animal models of respiratory syncytial virus pathogenesis and vaccine development: opportunities and future directions. In: Resch, B. (Ed.), Human Respiratory Syncytial Virus Infection. InTech978-953-307-718-5, .
Zappia, C.D., Soto, A., Granja-Galeano, G., Fenoy, I., Fernandez, N., Davio, C.A., Shayo, C., Fitzsimons, C.P., Goldman, A., Monczor, F., 2019. Azelastine potentiates anti-asthmatic dexamethasone effect on a murine asthma model. Pharmacol. Res. Perspect. 29 (6), e00531. https://doi.org/10.1002/prp2.531. 7.
Zhang, X., Chentoufi, A.A., Dasgupta, G., Nesburn, A.B., Wu, M., Zhu, X., Carpenter, D., Wechsler, S.L., You, S., BenMohamed, L., 2009. A genital tract peptide epitope vaccine targeting TLR-2 efficiently induces local and systemic CD8 + T cells and protects against herpes simplex virus type 2 challenge. Mucosal Immunol. 2 (2), 129–143.